MEDWIN PUBLISHERS
Committed to create value for Researchers

Open Access Journal of Waste Management & Xenobiotics
ISSN: 2640-2718

Comprehensive Model to Predict the Yield of the Pyrolysis Products of Kraft Lignin Based on Lumped Approach

Sherif Elshokary[1,*], Sherif Farag[1,2] and Bitu Hurisso[3]

[1]Faculty of Engineering at El-Mattaria, Helwan University, Cairo, Egypt

[2]Ecole Polytechnique Montreal, Canada

[3]Chemistry Department, Saint Mary's University, Halifax, Canada

Research Article

Volume 2 Issue 3

Received Date: August 03, 2019

Published Date: September 06, 2019

DOI: 10.23880/oajwx-16000127

***Corresponding author:** Sherif Elshokary, Faculty of Engineering at El-Mattaria, Helwan University, Cairo, Egypt, Tel: +201020002590; Email: sherifelshokary@gmail.com

Abstract

This work presents a comprehensive model based on the lumping approach to quantitively predict the products of the pyrolysis of kraft lignin. The yield of the primary pyrolysis products-biochar, bio-oil, and biogas-that are produced from the thermal decomposition of the lignin network are estimated. Different pyrolysis conditions and raw material characteristics are considered. The impacts of the particle size of the raw material, pyrolysis heating rate, and reaction residence time are taken into the investigation. The comparison of the predicted results using the developed model against the experimental data showed the high capability of the presented models to predict the biochar, bio-oil, and biogas yield under the examined conditions.

Keywords: Conventional Pyrolysis; Kraft Lignin; Bio-Oil; Pyrolysis; Lumped Approach

Introduction

Lignocellulosic biomass is composed of three intertwined main components: cellulose, 35-45 wt. %, hemicellulose, 25-30 wt. %; and lignin, 20-30 wt. %, all are on the dry basis [1-3]. In the pulping paper process, lignin is separated from the wood chips in the digestion step; where the wood chips and an aqueous solution – such as sodium hydroxide or sodium sulfide – are cooked at a certain pressure and temperature conditions. Lignin and other organic acids are produced in the form of white liquor and leave the digester at a solid concentration of 15-20 wt. %. White liquor is called black liquor after passing through a set of filtrates and evaporator trains. The other two components, which are called wood fibers, eventually become paper [1,4-6]. The most common industrial technique deals with black liquor aims to burn the material in a recovery boiler to recycle the inorganic chemicals and produce heat energy for the site. During the last few years, the growth in pulp production has led to reaching the design limit of the calorific load of the recovery boilers. The reason is that it is impossible to increase the pulp and paper production without the investment in expanding the capacity of the recovery boilers, which is an expensive solution [4,7]. Therefore, recover the cooking chemicals of the pulp and paper processes through the precipitation of lignin has widely been established in several locations. This methodology is

performed by the acidification, filtration, oxidization, and washing of black liquor.

Lignin is the only renewable source of aromatics in nature and considered the third-most abundant natural polymer after cellulose and hemicellulose. Lignin is an amorphous polymer consisting of phenylpropane units, originating from three aromatic alcohol precursors, p-coumaryl, coniferyl and sinapyl alcohol, as shown in Figure 1 [8-11]. The estimated annual production of lignin in US pulp and paper industry is over 50 million tons. About 2% of this quantity is converted to bio-products, whereas the rest is combusted to recover energy and chemicals [12].

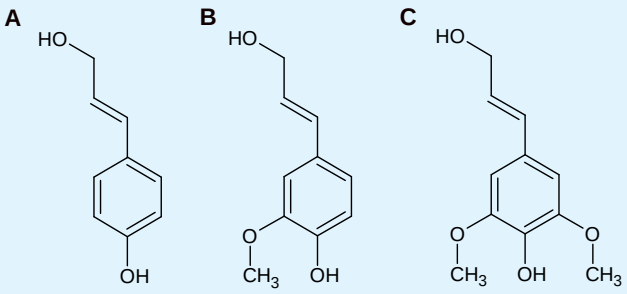

Figure 1: (A) coumaryl alcohol, (B) coniferyl alcohol, and (C) sinapyl alcohol.

Developing a platform to produce lignin-based intermediate/end-products beside the traditional commodities of the forest industry would enhance the bio-economics sector. Specifically, it could help in overcoming the challenges faced by the forest industry in North America during the last two decades. One of the most available techniques that can achieve this objective and accept the massive amount of lignin produced worldwide is the thermochemical decomposition (pyrolysis). It leads to decompose the chemical bonds of the feedstock by heating the payload in an oxygen-free environment. This technique produces three main products [8,13-15]:

- Solid, which is mostly carbon and can be used as a solid fuel, soil additive, in as a filler material in the tires industry, etc.;
- Condensable gas, which is primarily aromatics and a potential source of value-added chemicals; and
- Non-condensable gas, which is combustible.

Characterization of the pyrolysis lignin products has been well investigated in the scientific literature. Farag, et al. have investigated the effect of the microwave irradiation power on the chemical composition of bio-oil from pyrolysis of lignin using GC-MS, GC-FID, ^{13}C NMR, and ^{31}P NMR [2,16]. Pyrolysis-gas chromatography/mass spectrometry system (Py-GC-MS) was used by Lou et al. to study the effect of temperature and catalysts (sodium chloride and permutite) on the pyrolysis of bamboo lignin [17]. The same technique was performed by Jiang et al. to examine the temperature dependence of the composition of lignin pyrolysis products [18]. Zheng, et al. have also investigated the fast pyrolysis of lignin under the catalytic effect of $Mo_2N/\gamma\text{-}Al_2O_3$, using Py-GC-MS [19]. The pyrolysis of prairie cordgrass, aspen, and synthetic kraft lignin was investigated by Zhang, et al. using Py-GC-MS and TGA/FTIR. GC-MS/GC-FID [20]. Choi and Meier have examined the impact of the pyrolysis temperatures and catalyst (Zeolite HZSM-5, FCC, and Olivine) loading on the liquid product from the pyrolysis of kraft lignin [21]. GC-MS was performed on the lignin pyrolysis oil by De Wild et al. to quantitatively and qualitatively investigate the pyrolysis of lignin from two different biomass sources using a fluidized bed reactor [8]. TGA-FTIR was used by Luo, et al. to study the thermal behavior of organosolv lignin under the catalytic effect of zeolites [22].

Although considerable efforts have been made to better understand the influence of the pyrolysis parameters on the yield and composition of the products, less attention has been directed to model the lignin-based products based on a kinetic study. Therefore, this work aims to simulate the yield of the main three pyrolysis products, bio-oil, biochar, and biogas, using the kinetic parameters documented by Farag, et al. [12]. Such investigations would lead at providing insights toward achieving a desirable end-product yield and quality.

Raw Material

The raw material employed in this work was softwood kraft lignin. As documented by Farag, et al. [12], this material is precipitated from a Canadian kraft mill using The Ligno Force System™ a patent pending process. The CHNS elemental analysis of the material: C=63.27%, H=5.79%, N=0.07%, and S=1.56%, and the proximate analysis: Fixed carbon=37%, volatiles=62%, and ash=1% [16,23,24]. Further analysis such as ^{13}C and ^{31}P NMR for the virgin material can be found in the references [2,23]. The kinetic parameters associated with the reactions that produce the main three pyrolysis products from the raw material were obtained from the research article published by Farag, et al. [12], as shown in Table 1, the physical properties were considered as 0.1 W m^{-1} K^{-1} for

the effective thermal conductivity, 2.4 kJ kg^{-1} K^{-1} for the effective heat transfer coefficient, and 700 kg m^{-3} for the raw material density.

Product	k_o [min^{-1}]	E_a [kJ/mol]	n
Biochar	7	19	1
Bio-oil	22	29	1
Biogas	6	22	1

Table 1: The estimated kinetic parameters reported by Farag, et al. [12].

Governing Model

A spherical particle of lignin at different diameters was considered in this work. The particle is exposed to a superficial heating mechanism to increase the temperature to the decomposition point. Therefore, the particle is governed by three mechanisms of physics: reaction kinetics, heat transfer, and mass transfer.

Reaction Kinetics

Three parallel elementary reactions model were considered. The first reaction is to produce the biochar, which is the remaining solid as it is complicated to distinguish between the un-reacted material and the redacted portion. The other two reactions are the production of the bio-oil and the biogas. The kinetic reaction equations are listed below. Equation (1) for the remaining solid product while Equations (3) and (5) are for the bio-oil and biogas, respectively.

$$\frac{dc}{dt} = -A_c\,(c - c_\infty)^{n_c} \quad (1)$$

$$A_c = k_c\left(e^{\frac{-E_c}{RT}}\right) \quad (2)$$

$$\frac{dg}{dt} = A_g\,(c - c_\infty)^{n_g} \quad (3)$$

$$A_g = k_g\left(e^{\frac{-E_g}{RT}}\right) \quad (4)$$

$$\frac{do}{dt} = A_o\,(c - c_\infty)^{n_o} \quad (5)$$

$$A_o = k_o\left(e^{\frac{-E_o}{RT}}\right) \quad (6)$$

$$-\frac{dc}{dt} = \frac{dg}{dt} + \frac{do}{dt} \quad (7)$$

A_c refers to the reaction rate constant of the biochar product while A_o and A_g are for the bio-oil and biogas, which are defined in equations (2), (4), and (6); respectively. k_c, k_o, and k_g are the pre-exponential factor of the solid, liquid, and gas products, respectively [$time^{-1}$]. E is the apparent activation energy [J mol^{-1} K^{-1}], T is the reaction temperature [K], R is the universal gas constant [J mol^{-1} K^{-1}]. As explained above the subscript c, o, and g refer to the yield of the solid, liquid and gas at any time/temperature, respectively. c_∞ is the final solid yield that measured at the final temperature of the decomposition reaction, kindly refer to the proximate analyses mentioned above. The general mass balance equation is expressed in Equation (7).

Heat and Mass Transfer

Equation (8) represents the conservation of energy of heated material assuming all phases are at thermal equilibrium.

$$(\rho C)_{eff}\frac{\partial T}{\partial t} + \rho_g C_g u.\nabla T + \nabla.q = Q_{vd} + Q \quad (8)$$

$$\nabla.q = -\nabla.(k_{eff}\nabla T) \quad (9)$$

$$Q_{vd} = \left(\frac{dg}{dt}\Delta h_o^0 + \frac{dg}{dt}\Delta h_g^0\right)\rho_{c_0} \quad (10)$$

$$(\rho C)_{eff} = (1-\emptyset)\rho_c C_c + \emptyset\rho_g C_g \quad (11)$$

The term $(\rho C)_{eff}$ is the effective volumetric heat capacity of the solid, liquid, and gas (J/(m^3·K)) and Q is the heat source (W/m^3). ρ is the fluid density (kg/m^3), C is the fluid heat capacity at constant pressure (J/(kg·K)). Δh_o^0 is the heat of reaction of lignin conversion to condensable gas. Δh_g^0 is the heat of reaction of lignin conversion to non-condensable gas. ∅ is the porosity of the solid material. k_{eff} is the effective thermal conductivity is given by (W/(m·K)).

Equation (12) describes the chemical species transport. c_i is the concentration (mol/m^3), D_i the diffusion coefficient (m^2/s), and R_i is a reaction rate expression (mol/(m^3·s)) of the species i. u is the fluid velocity, the volume flow rate per unit cross-sectional area (m/s). The flux vector N (mol/(m^2·s)) is associated with the mass balance equation and used in boundary conditions and flux computations

$$\frac{\partial c_i}{\partial t} + \nabla.(-D_i\nabla c_i) + u.\nabla c_i = R_i \quad (12)$$

$$N_i = (-D_i\nabla c_i) + uc_i \quad (13)$$

$$\frac{\partial \rho_S}{\partial t} = -\left(\frac{do}{dt} + \frac{dg}{dt}\right) * \rho_{S_0} \quad (14)$$

$$\frac{\partial \emptyset\rho_o}{\partial t} + \frac{\partial \rho_o u}{\partial x} + \frac{\partial \rho_o v}{\partial y} + \frac{\partial \rho_o w}{\partial z} = \frac{do}{dt} * \rho_{c_0} \quad (15)$$

$$\frac{\partial \emptyset\rho_g}{\partial t} + \frac{\partial \rho_g u}{\partial x} + \frac{\partial \rho_g v}{\partial y} + \frac{\partial \rho_g w}{\partial z} = \frac{dg}{dt} * \rho_{c_0} \quad (16)$$

$$\emptyset = 1 - \rho_c/c_0(1 - \emptyset_0) \quad (17)$$

where ρ_c, ρ_o, ρ_g are the densities of remaining solid, liquid and the non-condensable gas and $\emptyset$ is the material porosity.

Results

Upon entering the system geometry and defining the boundary and initial conditions in the solver software, the selected element was governed by the reaction kinetics, and the heat and mass transfer characteristics. The time-dependent solver algorithm applied the Finite Element Method to solve all the equations. The time range was from 0 to 300 s with a step of 60 s. Relative and absolute tolerances were 0.01 and 0.001 respectively, and the number of the solved degrees of freedom was $13x10^4$.

Impact of the Particle Size

To examine the impact of the particle size of the pyrolyzed material on the temperature gradient and the product yield, three different particle diameters were investigated: 2 mm, 4 mm, and 10 mm. Figure 2 demonstrates the temperature gradients with in the lignin particle under investigation at each of these diameters.

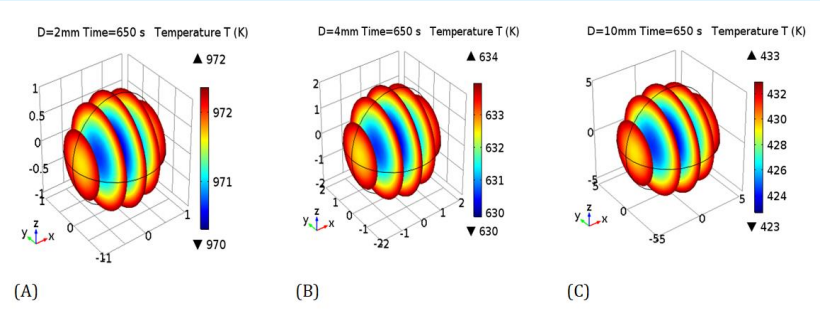

Figure 2: Temperature distribution within a lignin particle with a diameter of (A) 2 mm, (B) 4 mm, and (C) 10mm.

A temperature difference between the core and the surface of 10°C, 5°C, and 1°C was found after 650 s of the heating period for the 10 mm, 4 mm, and 2 mm of particle diameter, respectively. Indeed, such temperature differences, especially the higher one, would enhance initiating secondary reactions that would lead to further decompositions for the pyrolysis vapor. Pyrolysis vapor produced from the layers away from the surface must pass through the surface, which is at higher temperatures than the core, refer to Figure 3. As a result, the product selectivity will negatively be impacted because of the potential of such undesirable secondary reactions.

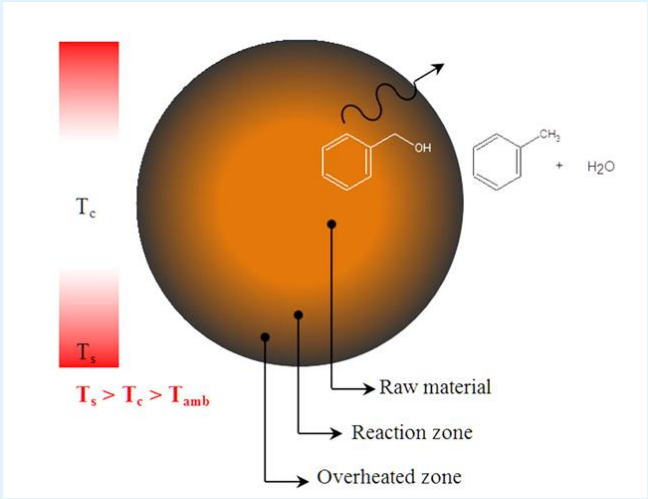

Figure 3: Impact of the temperature gradient on the product selectivity (Reprinted from reference [16]).

Figure 4 presents the transient yield of the produced biochar, bio-oil, and biogas of the three investigated particle diameters. As one see, pyrolysis starts on the outer surface toward the core of the particle. Thus, the remaining solid yield is found higher in the core compared to the surface. On the other hand, the transient bio-oil and biogas yields are much higher at the surface compared to the core.

Increase the particle diameter leads to boost the heat transfer limitation and, thus, yields more solid yield than the other two products. For example, 40 mol/m^3 of biochar yield was found in the case of 2 mm particle diameter compared to 67 mol/m^3, and 91 mol/m^3 in the cases of 4 mm and 10 mm diameters, respectively. The decomposition of the lignin side chains mainly produces gas and unsaturated bonds, which needs less heat energy than the decomposition of two aromatic compounds. Since increasing the particle size limits heat transfer into the core of the investigated particle, less energy will be provided to the chemical bonds. As a result, a noticeable decrease in the liquid yield while less change in the gas yield should be expected. For instance, an average liquid yield of 34mol/m^3, 11mol/m^3, and 1 mol/m^3 was found in the case of 2 mm, 4 mm, and 10 mm, respectively. An average biogas yield of 27mol/m^3, 22mol/m^3, and 8mol/m^3 was found in the case of 2 mm, 4 mm, and 10 mm, respectively. In other words, the liquid yield losses 96% and the gas yield losses 70 % of the base case when the diameter increased from 2mm to 10 mm.

To sum up, although increasing the particle diameter, within the examined range, was not very important from the heat, transfer aspect, it negatively impacts the liquid and gas yields.

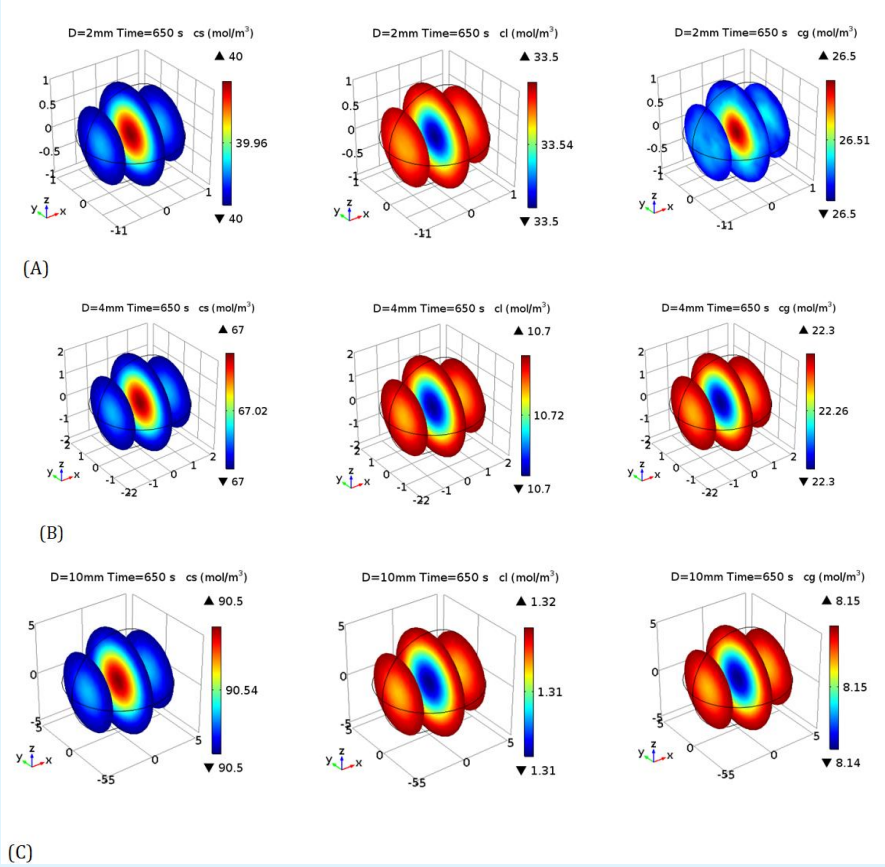

Figure 4: Solid (cs, left), liquid(cl, middle), and gas (cg, right) yield (in mol/m^3) of a lignin particle with a diameter of (A) 2 mm, (B) 4mm, and (C) 10mm.

Impact of the Heating Rate

The heating rate is one of the critical parameters that dramatically impact the liquid yield. Different heating rates have been considered in this work: 10°C/min, 36°C/min, and 104°C/ min, as shown in Figure 5. In the case of 2 mm of particle diameter, the impact of the heating rate is not apparent; however, the impact is significant in the average temperature, which is 380°C, 670°C, and 1400°C for the three applied heating rates, respectively.

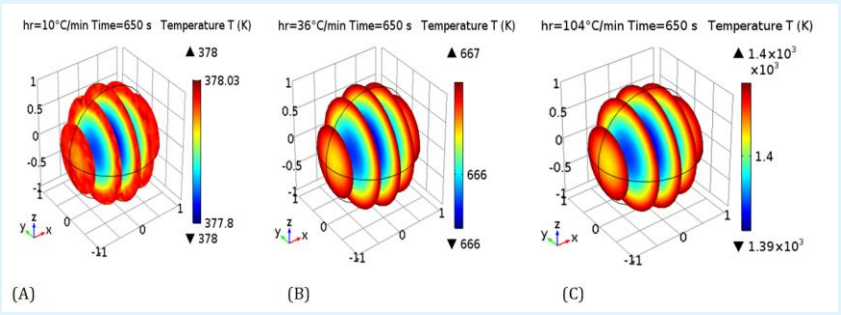

Figure 5: Temperature distribution of the lignin particle at different heating rates: (A) 10°C/min, (B) 36°C/min, and (C) 104°C/min.

Figure 6 shows the solid, liquid, and gas products at the heating rate of 10°C/min, 36°C/min, 56°C/min, 80°C/min, and 104°C/min after 650 s of heating. The overall view of the figure concludes that increasing the heating rate leads to increase the liquid product and decreasing the remaining solid. When the heating rate increased from 10°C/min to 56°C/min, the biochar yield decreased from 94 mol/m³ to 44 mol/m³ while the bio-oil yield increased from 0.6 mol/m³ to 29 mol/m³. Biogas yield followed the same trend of increasing as the bio-oil, where it increased from 5 mol/m³ to 27 mol/m³ within the same increase in the heating rate. As soon as the heating rate has increased from 56°C/min to 80°C/min and then to 104 °C/min, a significant decrease in the biogas is recognized, from 27 mol/m³ to 24 mol/m³ and then to 20 mol/m³, respectively. On the other hand, the biochar kept decreasing to 35 mol/m³, and the bio-oil increased to 45 mol/m³ at 104°C/min.

Decreasing the heating rate leads to produce a more solid product as the result of the slow pyrolysis. It mainly decomposes the side chains of the lignin network, which process more gas. Therefore, at 10°C/min, the gas yield was higher than the liquid yield. Increasing the heating rate provides the heat energy needed to decompose the lignin network for the production of liquid. After specific heating rate – in this case it is around 56°C/min-the time needed for the decomposition that produces a gas product decreased and, as a result, the gas yield is decreased.

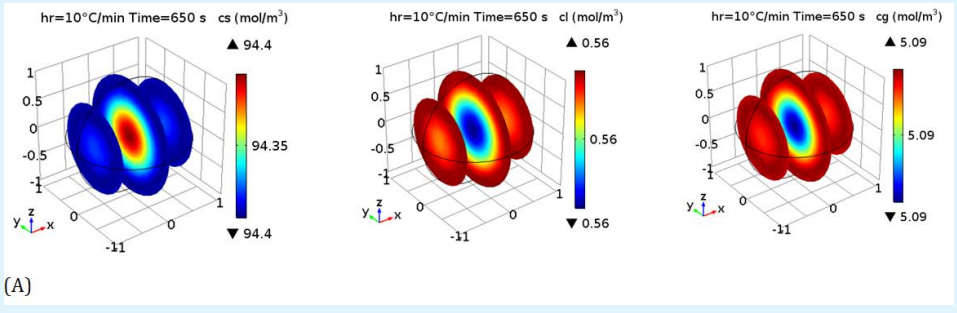

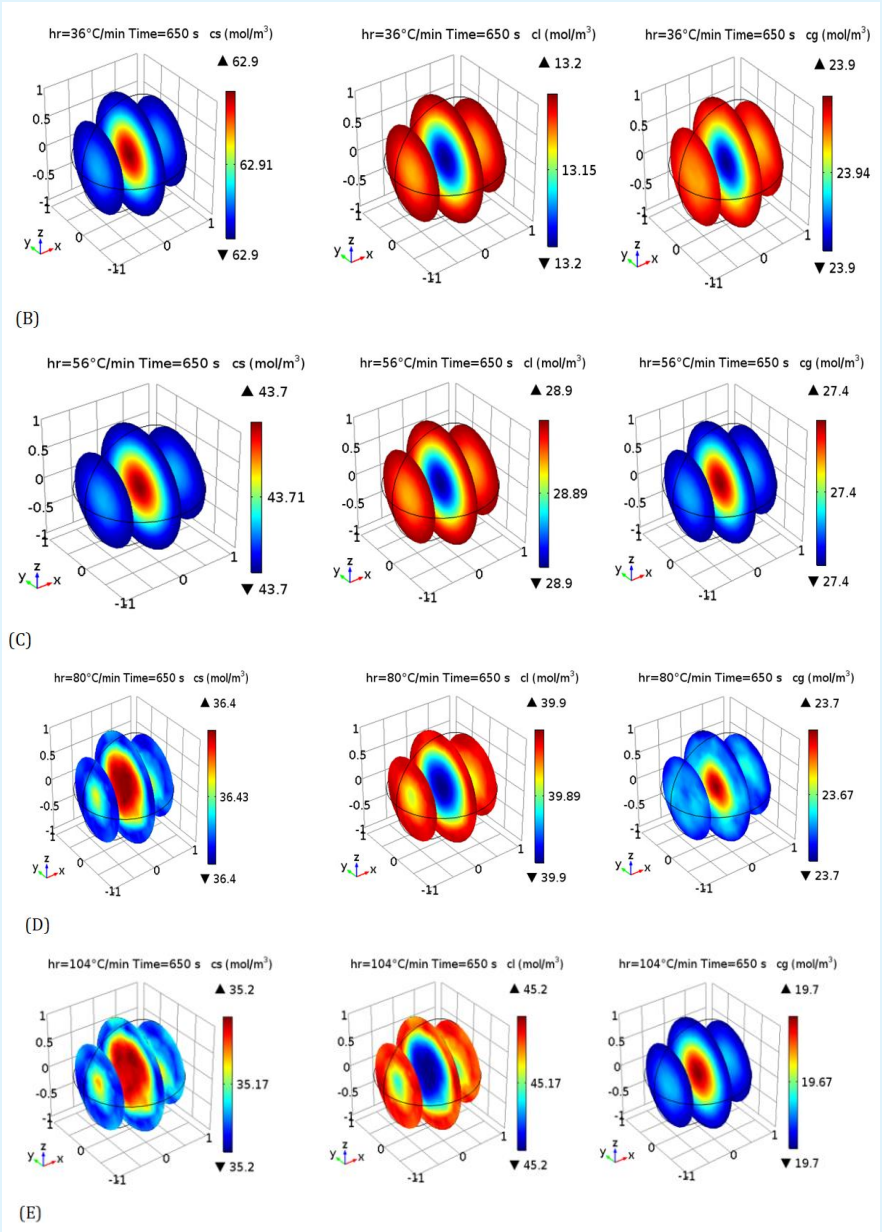

Figure 6: Solid (cs), liquid (cl), and gas (cg) yields of different heating rates: (A) 10°C/min, (B) 36°C/min, (C) 56°C/min, (D) 80°C/min, and (E) 104°C/min.

Impact of the Residence Time

Residence time is one of the critical parameters that impact the liquid yield and, most importantly, the product quality. To better understand the impact of this aspect, different residence times have been applied: 200 s, 400 s, and 600 s. Figure 7 demonstrates the impacts on the temperature distribution of the selected smaller particle diameter, 2 mm. At such a low particle size and long residence time, there almost no impact on the temperature gradients. This means that longer residence time leads to uniform distribution of temperature. The impact on the pyrolysis products based on the quantitative and qualitative aspects should be more visible.

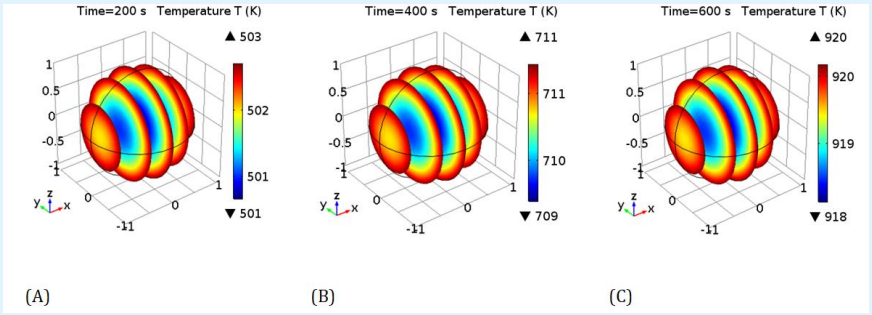

Figure 7: Temperature distribution of the lignin particle at different residence time: (A) 200s, (B) 400s, and (C) 600s.

Figure 8 exhibits the yield of the pyrolysis products of different residence times: 200 s, 400 s, 600 s, and 800 s. It should be noted that increasing the residence time could enhance the secondary reaction that takes place meanwhile the pyrolysis process. Such undesirable reactions would lead to further decomposition for the pyrolysis vapor and, thus, increase the biogas yield. In this work, it was difficult to include the kinetics of the secondary reactions of the pyrolysis vapor since it is out of the scope of the work and its kinetics information is insufficient in the literature. The primary purpose of this aspect is to understand better the maximum time that is enough to reach the complete conversion. As it is clear from the figure after 600 s there is no noticeable change in the yield of the solid, liquid, and gas products. Therefore, there is no point behind heating the feedstock for more time, which is not acceptable from the process economics point of view.

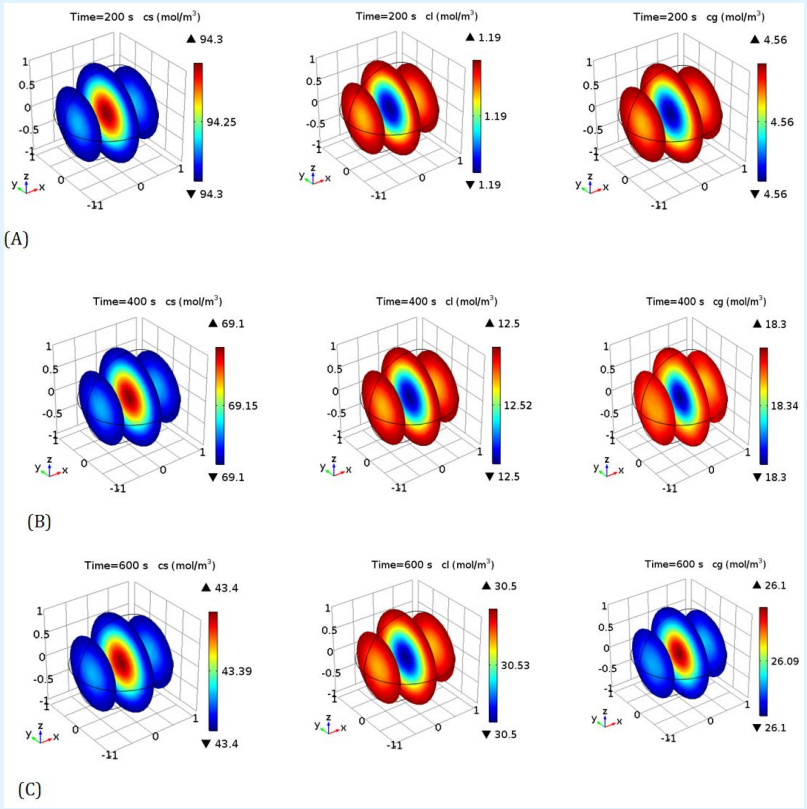

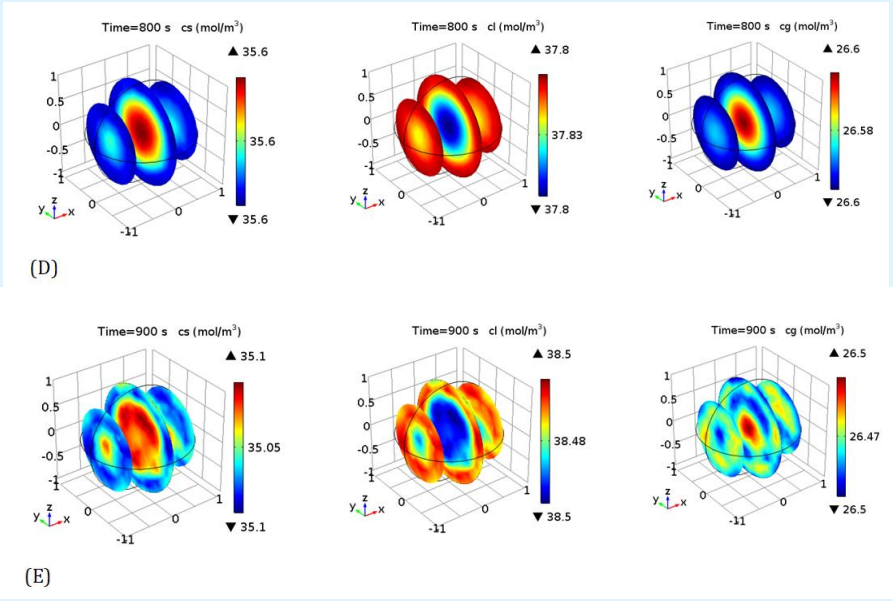

Figure 8: Solid (cs), liquid(cl), and gas (cg) yields of different residence times: (A) 200 s, (B) 400 s, (C) 600 s, (D) 800 s and (E) 900s.

Volume Average Product Yield

The product yield of the investigated particle was integrated and, then, the average volume yield of the solid, liquid, and gas products was calculated and presented in Figure 9. The complete conversion of the materials was done at 1050 K, which is relatively high compared to that of the other biomass components, cellulose, and hemicellulose. The reason behind this aspect is the complex structure of the lignin network. Theoretically, the thermal degradation of lignin starts at 400 K, which is mainly for the decomposition of the side chains that mainly produce water, gas, and/or unsaturated chains. The decomposition of lignin takes place over a wide temperature range from 400 K to 1050 K for its complicated structure.

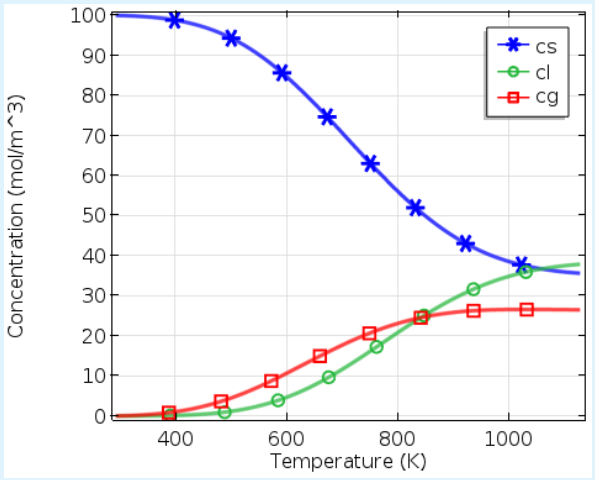

Figure 9: Volume Average product yield.

Model Validation

The results obtained from the model presented in this work were validated against the experimental data developed by Farag et al. and published in reference [12]. In that reference significant modifications were done to make a traditional microwave oven working as a thermogravimetric analyzer – the authors called it MW-TGA. As shown in Figure 10, the pyrolysis reactor connected to a weight balance to precisely measure the weight of the reacted material(s) during the electromagnetic irradiation. An innovative thermometer – called an air-thermometer, and does not suffer from the drawbacks of traditional thermometers in the presence of microwaves- was employed to measure the transient bulk temperature of the payload. A product manifold of seven ports used to splitting the pyrolysis vapor at different times or temperatures for recording the transient solid, liquid, and gas yields for the kinetic purposes. For further details regarding this developed MW-TGA, kindly refer to references [2,12,16,25].

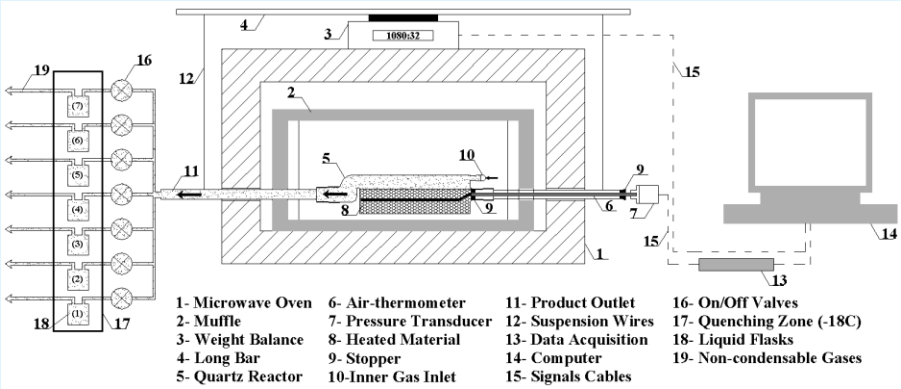

Figure 10: Microwave thermo-gravimetric analyzer with a product manifold (Reprinted from reference [12]).

As it is evident in Figure 11, the presented models have a high capability to estimate the solid, liquid, and gas yield of the products with minor deviations. This means that these three models can be applied in designing and scaling-up the pyrolysis process, which is essential for the industrial applications.

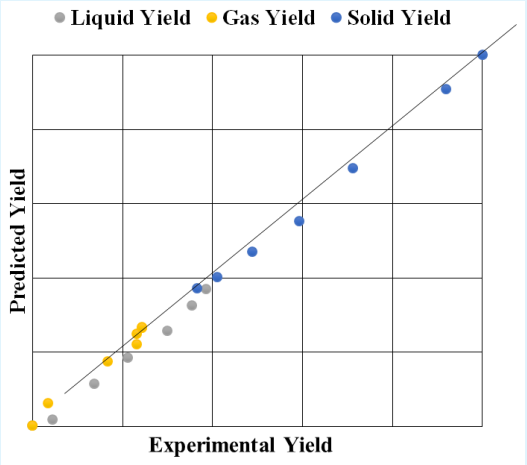

Figure 11: The capability of the presented models.

Conclusion

A three-dimensional mathematical model based on lumped approach to predict the products from pyrolysis of kraft lignin was developed. The influences of the raw material particle size, decomposition heating rate, and pyrolysis residence time were investigated. The key findings of the work include:

- The thermal decomposition of lignin takes place over a wide temperature range- from 400 K to 1050 K for its complex structure;
- The yield of the solid product at the core of the lignin particle is higher than that of the surface;
- The transient liquid and gas yields at the surface of the particle are much higher than the core;
- Increase the particle diameter prompts the heat transfer limitations and, consequently, produces more solid than the liquid and gas;
- Decrease the heating rate leads to producing more solid as the result of the slow pyrolysis, which mainly decomposes the side chains of the lignin network; and
- Increase the residence time enhances the secondary reactions that take place meanwhile the pyrolysis process, leading to further decomposition for the pyrolysis vapor and, thus, increase the biogas yield.

Comparing the predicted result against the experimental data shows the high capability of the developed model to estimate the pyrolysis products with minor deviations.

References

1. Farag S (2013) Production of Chemicals by Microwave Thermal Treatment of Lignin, in Chem Eng University of Montreal: Ecole Polytechnique de Montreal.

2. Farag S, Fu D, Jessop PG, Chaouki J (2014) Detailed compositional analysis and structural investigation of a bio-oil from microwave pyrolysis of kraft lignin. Journal of Analytical and Applied Pyrolysis 109: 249-257.

3. Mudraboyina BP, Farag S, Banerjee A, Chaouki J, Jessop PG (2015) Supercritical Fluid Rectification of Lignin Pyrolysis Oil Methyl Ether (LOME) and Its Use as a Bio-derived Aprotic Solvent. Green Chemistry 18(7): 2089-2094.

4. Farag S, Chaouki J (2015) Economics evaluation for on-site pyrolysis of kraft lignin to value-added chemicals. Bioresource Technology 175: 254-261.

5. Kouisni L, Gagne A, Maki K, Holt-Hindle P, Paleologou M (2016) LignoForce System for the Recovery of Lignin from Black Liquor: Feedstock Options, Odor Profile, and Product Characterization. ACS Sustainable Chemistry & Engineering 4(10): 5152-5159.

6. Custodis VBF, Hemberger P, Ma Z, van Bokhoven JA (2014) Mechanism of Fast Pyrolysis of Lignin: Studying Model Compounds. The Journal of Physical Chemistry B 118(29): 8524-8531.

7. Farag S, Chaouki J (2015) Technical and Economic Feasibility of Pyrolysis of Kraft Lignin. In Materials for Oil, Gas & Biofuels Chapter 4, Materials for Energy, Efficiency and Sustainability: Tech Connect Briefs, Washington, DC.

8. de Wild PJ, Huijgen WJJ, Heeres HJ (2012) Pyrolysis of wheat straw-derived organosolv lignin. Journal of Analytical and Applied Pyrolysis 93: 95-103.

9. Zakzeski J, Bruijnincx PC, Jongerius AL, Weckhuysen BM (2010) The Catalytic Valorization of Lignin for the Production of Renewable Chemicals. Chemical Reviews 110(6): 3552-3599.

10. Kibet J, Khachatryan L, Dellinger B (2012) Molecular Products and Radicals from Pyrolysis of Lignin. Environmental Science & Technology 46(23): 12994-13001.

11. Samih S, Latifia M, Farag S, Leclerca P, Chaouki J (2018) From complex feedstocks to new processes: the role of the newly developed micro-reactors. Chemical Engineering and Processing-Process Intensification 131: 92-105.

12. Farag S, Kouisni L, Chaouki J (2014) Lumped Approach in Kinetic Modeling of Microwave Pyrolysis of Kraft Lignin. Energy & Fuels 28(2): 1406-1417.

13. Doucet J, Laviolette JP, Farag S, Chaouki J (2014) Distributed Microwave Pyrolysis of Domestic Waste. Waste and Biomass Valorization 5(1): 1-10.

14. Farag S, Chaouki J (2015) Microwave Heating Assisted Biorefinery of Biomass, in Innovative Solutions in Fluid-Particle Systems and Renewable Energy Management. IGI Global: Hershey, 131-166.

15. Samih S, Farag S, Chaouki J (2018) Innovative Microreactors for Low-grade Feedstock Gasification, Gasification for Low-grade Feedstock. IntechOpen.

16. Farag S, Mudraboyina BP, Jessop PG, Chaouki J (2016) Impact of the Heating Mechanism on the Yield and Composition of Bio-oil from Pyrolysis of Kraft Lignin. Biomass and Bioenergy 95: 344-353.

17. Lou R, Wu SB, Lv GJ (2010) Effect of conditions on fast pyrolysis of bamboo lignin. Journal of Analytical and Applied Pyrolysis 89(2): 191-196.

18. Jiang G, Nowakowski DJ, Bridgwater AV (2010) Effect of the Temperature on the Composition of Lignin Pyrolysis Products. Energy & Fuels 24(8): 4470-4475.

19. Zheng Y, Chen D, Zhu X (2013) Aromatic hydrocarbon production by the online catalytic cracking of lignin fast pyrolysis vapors using Mo2N/γ-Al2O3. Journal of Analytical and Applied Pyrolysis 104: 514-520.

20. Zhang M, Resende FLP, Moutsoglou A, Raynie DE (2012) Pyrolysis of lignin extracted from prairie cordgrass, aspen, and Kraft lignin by Py-GC/MS and TGA/FTIR. Journal of Analytical and Applied Pyrolysis 98: 65-71.

21. Choi HS, Meier D (2013) Fast pyrolysis of Kraft lignin-Vapor cracking over various fixed-bed catalysts. Journal of Analytical and Applied Pyrolysis 100: 207-212.

22. Luo Z, Wang S, Guo X (2012) Selective pyrolysis of Organosolv lignin over zeolites with product analysis by TG-FTIR. Journal of Analytical and Applied Pyrolysis 95: 112-117.

23. Fu D, Farag S, Banerjee A, Chaouki J, Jessop PG (2014) Extraction of phenols from lignin microwave-pyrolysis oil using a switchable hydrophilicity solvent. Bioresource Technology 154: 101-108.

24. Mudraboyina BP, Farag S, Banerjee A, Chaouki J, Jessop PG (2016) Supercritical fluid rectification of lignin pyrolysis oil methyl ether (LOME) and its use as a bio-derived aprotic solvent. Green Chemistry 18(7): 2089-2094.

25. Farag S, Chaouki J (2015) A modified microwave thermo-gravimetric-analyzer for kinetic purposes. Applied Thermal Engineering 75: 65-72.